Renewable and Sustainable Energy Reviews 52 (2015) 1668–1679

Contents lists available at ScienceDirect

Renewable and Sustainable Energy Reviews

journal homepage: www.elsevier.com/locate/rser

Stochastic optimization of hybrid renewable energy systems using sampling average method

Masoud Sharafi [a], Tarek Y. ElMekkawy [b,*]

[a] Department of Mechanical Engineering, University of Manitoba, Winnipeg, MB, Canada R3T 5V6
[b] Department of Mechanical and Industrial Engineering, Qatar University, Doha, Qatar

ARTICLE INFO

Article history:
Received 22 November 2014
Received in revised form
27 April 2015
Accepted 1 August 2015
Available online 29 August 2015

Keywords:
Stochastic multi-objective optimization
Hybrid renewable energy system
Near zero energy buildings

ABSTRACT

The stochastic attribute of renewable energy sources and the variability of energy load is a preeminent barrier to design hybrid renewable energy systems. In this paper, a new methodology is advanced to incorporate the uncertainties associated with RE resources and load in sizing an HRES in the application of buildings with low to high renewable energy ratio (RER). Dynamic multi-objective particle swarm optimization (DMOPSO) algorithm, simulation module, and sampling average technique are used to approximate a Pareto front (PF) for an HRES design through a multi-objective optimization framework. The main aim of design is to simultaneously minimize total net present cost (NPC), maximize renewable energy ratio, and minimize fuel emission while satisfy a desirable level of loss of load probability (LLP). The existing randomness in wind speed, solar irradiation, ambient temperature, and energy load is considered using synthetically data generation and sampling average method. The performance of the model has been examined in a building located in Canada as the case study, in which RER of the building is increased by using renewable energy technologies. The generated PF by the stochastic approach is compared to a deterministic PF using well-known performance metrics. Finally, a sensitivity analysis is carried out where the economic characteristics of the model are varied.

Contents

* Corresponding author. Tel.: +974 44034369; fax: +974 44034301.
E-mail address: tmekkawy@qu.edu.qa (T.Y. ElMekkawy).

http://dx.doi.org/10.1016/j.rser.2015.08.010
1364-0321/

Nomenclature

A(day) daily amplitude of temperatures [°C]
$a_{d,h}$ random number between 0 and 1
$A_{\text{mean},d}$ mean daily amplitude of temperature [°C]
$A_{\text{max},d}$ maximum daily amplitude of temperature [°C]
A_m monthly amplitude of wind speed [m/s]
$C_{b,\text{Col}}$ biomass collection cost [CAD/t]
$C_{b,\text{St}}$ biomass storage cost [CAD/t]
$C_{b,\text{Tr}}$ biomass transportation cost [CAD/t km]
$c_{d,h}$ correlated values for wind speed
$C_{\text{elec},s}$ electricity price sold to the grid [CAD/kW h]
$C_{\text{elec},b}$ electricity price bought from grid [CAD/kW h]
C_{Gas} gasoline price [CAD/l]
$C_{I,j}$ capital cost per unit for component j [CAD/unit]
C_{NG} natural gas price [CAD/m^3]
$C_{O\&M,j}$ operation and maintenance cost per unit for component j [CAD/unit]
$C_{\text{rep},j}$ replacement cost per unit for the component j [CAD/unit]
COE cost of energy
CRF capital recovery factor
DM diversification metric
d_m the number of days in a month
E_{EX} excess electricity should be sold or bought [kW h]
$El_{s,y}$ annual sold electricity to the grid [kW h/year]
E_{bought} bought electricity from the grid [kW h]
E_{AR} electricity consumption by air refrigerator [kW h]
E_{EV} electricity consumption by PEV [kW h]
E_{HP} electricity consumption by heat pump [kW h]
E_{Sold} sold electricity to the grid [kW h]
E_{PV} net power generated by PV panel [kW h]
$E_{\text{PV-Re}}$ PV panel power output [kW h]
$E_{\text{PVR-Re}}$ rural PV panel power output [kW h]
E_{WT} net power generated by wind turbine [kW h]
Load the total energy load over a year [kW h]
P_{Bio} biomass boiler capacity [kW]
P_{HP} heat pump capacity [kW]
P_{HST} heat storage tank capacity [m^3]
P_{SC} solar collector capacity [kW]
P_{PVR} rural PV panel capacity [kW]
P_{PV} PV panel capacity [kW]
P_{WT} wind turbine capacity [kW]
T_{base}(day) daily base temperature [°C]
$T_{\text{min},m}$ monthly averaged minimum ambient temperature [°C]
$T_{\text{max},m}$ monthly averaged maximum ambient temperature [°C]
$T_{\text{mean},m}$ monthly averaged mean ambient temperature [°C]
Unmet load unmet energy load over a year [kW h]
$w_{d,h}$ hourly wind speed [m/s]
$w_{\text{av},m}$ average monthly wind speed [m/s]
$w_{n,m}$ average monthly night speed [m/s]
Weibull$_{d,h}$ random number following a Weibull distribution
ε_h random number
$E_{\text{WT-Re}}$ wind turbine power output [kW h]
EF_E emission factor for grid electricity [kg CO_2/KW h]
EF_{Gas} emission factor for gasoline [kg CO_2/l]
EF_{NG} emission factor for NG [kg CO_2/m^3]
$El_{b,y}$ annual electricity bought from grid [kW h/year]
$f_{\text{correction-}m}$ correction factor
GAS hourly gasoline consumption [kW h]
Gasoline annual gasoline consumption [l/year]
$h_{\text{max},m}$ the hour of maximum daily speed [h]
HE_{Bio} heating load on biomass boiler [kW h]
HE_{HP} heating load on HP [kW h]
HE_{NG} heating energy generated by NG boiler [kW h]
$HP(t)$ hourly heat pump output [kW h]
$HST(t)$ level of hot water in storage tank in time step t [kW h]
$HW_{\text{Bio-tank}}$ hot water load on biomass boiler [kW h]
$HW_{\text{HP-tank}}$ hot water load on HP [kW h]
$HW_{\text{NG-tank}}$ hot water generated by NG boiler [kW h]
$HW_{\text{SC-tank}}$ hot water generated by SC [kW h]
$HW_{T-\text{load}}$ total hot water sent to load [kW h]
H_o(day) extraterrestrial solar radiation in a given day [kW h/m^2]
H_o(month) monthly averaged daily extraterrestrial solar radiation [kW h/m^2]
i Interest rate [%]
I_h hourly solar radiation [kW h/m^2]
$I_{\text{max},m}$ monthly average of maximum solar radiation for a day [kW h/m^2]
I_{max}(day) the maximum solar radiation for a day [kW h/m^2]
I_{max}(month) the maximum solar radiation in a month [kW h/m^2]
K single payment present worth
NPC net present cost
NPV net present value
LLP_{max} loss of load probability upper limit [%]
LLP loss of load probability [%]
PT temperature periodic term [°C]
RER renewable energy ratio [%]
SC set coverage metric
SD standard deviation
SM spacing metric
ST solar term of temperature [°C]
$T(t)$ hourly ambient temperature [°C]
T_{base} base term of temperature [°C]
T_{mean}(day) mean daily temperature [°C]
$\varepsilon_{\text{Tr,gas}}$ transportation allocation coefficient of gasoline car
$\varepsilon_{\text{Tr,PEV}}$ transportation allocation coefficient of PEV
$\varepsilon_{\text{CO,AR}}$ cooling allocation coefficient of air refrigerator
$\varepsilon_{\text{CO,HP}}$ cooling allocation coefficient of heat pump
$\varepsilon_{\text{HE,bb}}$ heating and hot water allocation coefficient of biomass boiler
$\varepsilon_{\text{HE,HP}}$ heating and hot water allocation coefficient for heat pump
θ_h the scale factor of Weibull distribution
$\mu_{d,h}$ average hourly solar radiation [kW h/m^2]
χ random variable with normal distribution function

1. Introduction

Looking for a sustainable environment restricts the fossil fuels consumption and consequently encourages the usage of renewable energy (RE) sources [1]. In fact, RE sources are becoming popular as their negative environmental impact are not significant in contrast to the fossil fuels [2–5]. Renewable energy is titled as clean energy sources by which greenhouse gas emission can be reduced and secondary wastes are generated at minimum level. In the future, renewable energy application is expected to increase since RE resources are local and environmental friendly. Furthermore, they can aid in cutting down the running of traditional fuels [1]. The application of hybrid renewable

energy systems (HRES) for remote area has attracted many attentions due to the rise in the prices of fossil fuels and the resultant advances in renewable energy technologies. Generally, an HRES includes two or more renewable energy sources integrated together to improve both power reliability and system efficiency.

The main challenge of the design of HRESs is the variability and availability of RE resources [6]. The performance of HRES is fluctuating drastically over years since the renewable resources can be distinct in terms of average values and distribution over years. Taking into account the randomness associated with RE resources and load is critical since it has significant effect on the reliability and the overall performance of HRESs. The reason for this fact is that system operation and produced power are dependent on the stochastic nature of RE sources. It is not easy to make the reliability analysis of an HRES without considering its probabilistic nature due to inherent uncertainties in renewable resources. In other words, employing reliability as an objective in the optimization of an HRES design cannot be executed deterministically [7]. In recent past, the advancement of probabilistic design methods has become more popular among the researchers due to the diagnosing of the drawback of deterministic methods in the design of HRES [7]. The design of such energy suppliers involves the approximation of the capacities of the generators and storage devices to fulfil a given demand. Stochastic approaches of sizing HRESs cover the issue of the RE variability in the system design [8].

A few researchers have carried out stochastic analysis of HRESs respecting to their performance and their design optimization. Table 1 summarizes the recent studies that applied stochastic analysis in HRESs design. Dufo-López et al. [9] studied the impact of the uncertainty of wind data on the optimal design of wind-batteries stand-alone systems by using hybrid optimization of genetic algorithm (HOGA). They considered two types of input data including measured hourly data and synthetically generated hourly wind speed data over a year. They implied that the main advantage of their approach is to consider a certain number of consecutive days of "calmness" for generating the wind speed data. Handschin et al. [10] proposed a "scenario-wise" approach to develop an engineering tool to optimize a coordinated operation of distributed generation (DG) units incorporating the uncertainties associated with electric load, power prices, and infeed from renewable resources. Arun et al. [8] utilized chance constrained programming based on the design space approach for the optimum sizing of an off-grid PV-battery system under the uncertainty of solar insolation. In their study, the set of all possible design configurations was illustrated by drawing a sizing curve in which a desirable confidence level is used to integrate the possible combinations of the PV sizes with the equivalent minimum battery capacities. Ekren et al. in [1,11] optimized the size of a hybrid energy system including PV/wind and battery storage employing two simulation-based optimization methods. The probabilistic distribution functions for solar radiation, wind speed and electricity consumption were fitted employing ARENA simulation software. Lastly, they applied response surface methodology (RSM) and the OptQuest tool in ARENA to optimize the total cost of the system. They extended their work in [12] to perform a Simulated Annealing (SA) algorithm for the optimal design of the HRES. They concluded that the SA algorithm gives better result than RSM approach. In [13], for the optimal design of a renewable power generation system, the uncertainties of weather data and the operating efficiency of the studied subsystems were addressed by using probability distribution function. The stochastic annealing optimization algorithm was used to minimize the economic objective. Khan et al. [14] represented the stochastic nature of wind speed and solar radiation level by using a sensitivity analysis approach. They performed a simulation study of a hybrid energy system for application in Canada. A renewable energy simulation software (HOMER) was used as a sizing tool to discuss the cost and the performance of renewable and non-renewable energy sources. Kuznia et al. [15] presented a stochastic mixed integer programming model to identify the optimal combination and the size of a hybrid system consisting randomness in wind speed and electricity load. They created a Benders' decomposition algorithm to obtain the optimal solution. Maheri [7] developed a multi-objective

Table 1
The summary of recent published studies for stochastic optimization of HRESs.

Authors	System components								MOP	Objective functions	Stochastic parameters	Optimization approach
	Wind turbine	PV panel	Solar Collector	Biomass	Heat Pump	PEV	Storage	Diesel & other				
Ekren et al. [1]	●	●					●		NO	NPC	Wind speed, Solar radiation, Electricity load	RSM/Simulation based Opt Quest in ARENA
Maheri [7]	●	●						●	YES	LCE Reliability	Wind speed, Solar radiation, Electricity load PV array efficiency	GA
Arun et al. [8]		●					●		NO	Energy cost	Solar insolation	Design space/Chance constrained programming
Dufo-López et al. [9]	●						●		NO	NPC	Wind speed	HOGA
Handschin et al. [10]	●	●						●	NO	Operation Cost	Power prices, Power load, In feed from RE	Scenario-wise MILP
Garyfallos et al. [13]	●	●					●	●	NO	NPV	Wind speed, Solar radiation, Efficiencies of EL and FC	SA
Khan et al. [14]	●	●					●	●	NO	NPC	Wind speed, Solar radiation, Diesel price, FC cost	Sensitivity analysis HOMER
Kuznia et al. [15]	●						●	●	NO	NPC	Wind speed/Electricity load	SMIP
Roy et al. [16]	●						●		NO	COE	Wind speed	Chance constraint programming/ Graphical method
Subramanyan et al. [17]								●	Yes	CO_2 emissions Capital cost Current density Overall efficiency	Fuel cell current density	MINSOOP/NLP/Sampling method
Wang [18]	●	●					●	●	Yes	NPCReliability Emission	Wind speed, Solar radiation, Electricity load	Generating scenarios/MOPSO

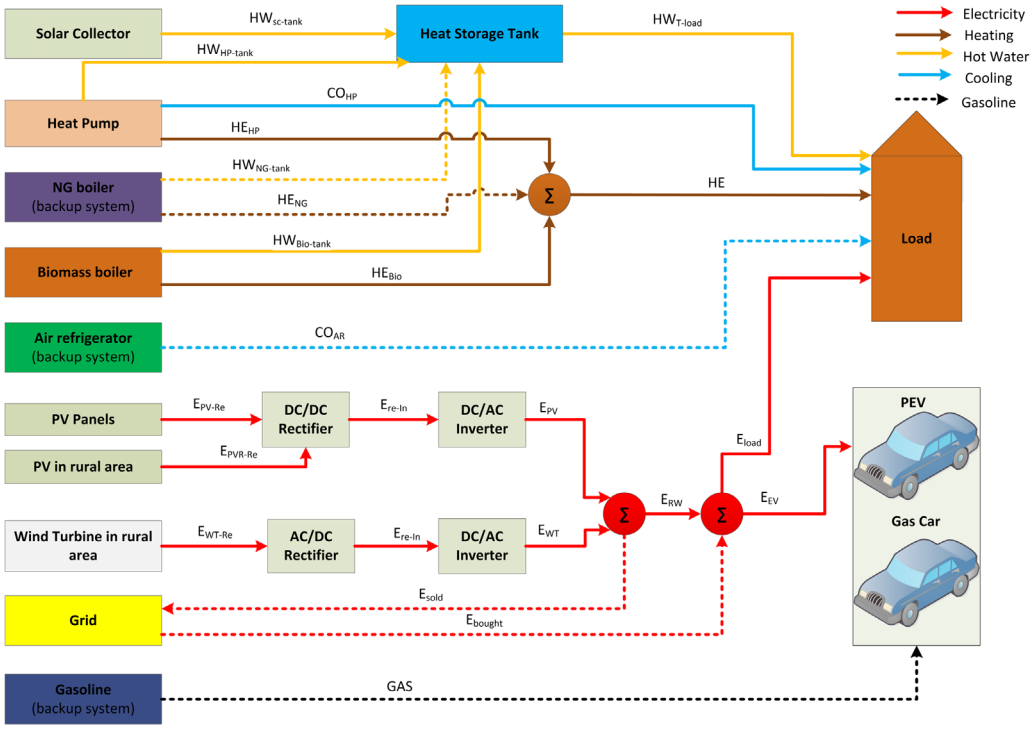

Fig. 1. Energy flow in the proposed hybrid renewable energy system [19].

optimization method for design under uncertainty of a wind-PV-diesel configuration. The probabilistic analysis was used to quantify the system reliability since there are uncertainties in renewable resources and electricity demand. To tackle the uncertainties, only the uniform distribution function was fitted to all random parameters. Roy et al. [16] developed a chance constrained programming technique to design an off-grid wind-battery system incorporating uncertainty in wind speed. In their study, Monte-Carlo simulation approach validated the system reliability where the hourly wind speed was modeled as Weibull random variable, and the cost of energy was selected as design criteria to evaluate the proposed system configuration. Subramanyan et al. [17] used MINSOOP, NLP optimizer, and sampling techniques to pass the Pareto set for the design of a solid oxide-proton exchange membrane fuel cell (SOFC–PEM) by means of a multi-objective optimization framework. The existing randomness in fuel cell current density was modeled to convert the approach to a stochastic multi-objective optimization one. Wang [18] presented multi-criteria meta-heuristic method to design an HRES including a wind turbine and PV panels according to cost, reliability, and emission criteria. Adequacy evaluation was performed to consider system uncertainties based on the primarily defined scenarios.

In summary, few articles used stochastic analysis for the design of HRESs. However, persisted researches and development are still required to improve these systems sizing process. Most of the previous studies have only considered economic objectives at the design stage (see Table 1) while it is very important to size an HRES based on pollutant emission, reliability, and renewable energy ratio. In addition, they neglected simultaneously providing energy for heating, cooling, and appliances. Furthermore, mostly in the previous studies, the random parameters are generated using a simple distribution function.

In this paper, a new stochastic multi-objective approach is developed to incorporate the existing uncertainties in RE resource and energy load when sizing an energy supply system. The proposed methodology is trying to simultaneously examine the economic, reliability, and environmental issues for different renewable energy ratio (RER). This study is the extension of the previous work of the authors [19] with difference in involving the stochastic evaluation instead of using a deterministic design approach. The contribution of the present work is that a comprehensive energy supply system is studied incorporating uncertainties in RE resources and energy load. Moreover, similar to the previous work [19], the transport load is considered rather than electricity, heating, and cooling load. Additionally, simple methods for synthetic generation of daily load profile and weather data has been applied to handle the existing uncertainties in the model.

Mostly, in the probabilistic analysis of HRES designs, an objective function cannot be evaluated exactly but rather approximation methods are required. In this study, the sampling average approximation is integrated with dynamic multi-objective particle swarm optimization algorithm (DMOPSO) to help in handling the complex optimization problem. The generated solutions by the implemented approach are evaluated by comparing with the solutions obtained by deterministic analysis. Then, a sensitivity analysis is carried out to identify the economic parameters that have significant impact on the design objectives. Based on the best authors' knowledge, it is the first time a MOP approach incorporating a comprehensive stochastic analysis is implemented for the optimal design of a renewable energy supply system in the application of low energy buildings. In other words, it is the first time, the randomness in wind speed, solar radiation, ambient temperature, electricity load, heating and cooling load, hot water demand (HWD), and transportation load are simultaneously considered in the sizing of HRESs.

Section 2 explains the problem description. Section 3 begins with the definition of considered objective functions in the proposed design methodology, and then elaborates on the sampling average approach and the synthetic generation of random parameters. Section 4 describes a summary of the employed DMOPSO algorithm. Section 5 details the design scenarios and

the results of the case study that is delivered by using the proposed design methodology.

2. Problem description

A hypothetical grid-connected hybrid renewable energy system including renewable and non-renewable energy conversion technology is chosen as our case study. This HRES is used to increase the renewable energy ratio of a building located in Canada. As shown in Fig. 1, this energy system may employ wind turbines, PV panels, solar thermal collectors, heat pumps, biomass boilers and heat storage tanks [19]. The employed renewable energy technologies are supposed to provide energy for electricity, heating, and cooling load. The employed backup systems such as grid and natural gas (NG) boiler help to supply the energy demand when the considered RE sources are not able to satisfy the required energy. In a city like Winnipeg, it is not legal to install a wind turbine in the city area. For this reason, it is assumed that wind turbines would be installed in the rural area of the city and its electricity can be easily sold to the grid. The rural area is supposed to be located in area that the electrical grid is established. Thus, there is no limitation to connect the employed wind turbines and PV panels to the grid and selling their produced electricity to the grid. In this study, as it is assumed that the employed system meets the technical requirements [20], it is possible to export electricity to the grid. In Fig. 1, two alternative locations for PV panel installation are designed; it can be installed either on the top of the building roof or in the rural area. There are two options to meet required transportation of the building: using plug-in electric vehicle (PEV) or gasoline car. It is assumed that the energy required for PEV is met by electricity, if there is no enough electricity, the gasoline will be used to guarantee the load. A heat pump or air refrigerators will cover the cooling load through summers.

It is intended to find the optimal configuration and optimal size of the employed technologies such that simultaneously minimize the total net present cost (NPC) of the system for entire life time of the system, minimize annual CO_2 emission, and maximize RER while satisfying a certain level of reliability.

Moreover, there is uncertainty in weather data (wind speed, solar radiation, and ambient temperature) and energy load. These uncertainties have significant effect on the design space. The main aim of this study is to establish a methodology to deal with uncertainties existing in the design process of this type of energy supply system. In other words, the developed approach returns best combination of employed technologies and their corresponding optimal size while considering randomness existing within input data. For this purpose, the design problem is formulated as a stochastic multi-objective optimization problem including three objective functions. In this regards, RE resources data, heating, cooling, and electricity load profile on an hourly basis are generated by using the most common models, see Section 3.2. To specify employed technologies, their actual cost data is considered as well as their mathematical models and the technical structures are stated. Based on these data, the three objective functions are optimized with respect to the energy balance equations as well as other technical constraints. In order to solve the complex optimization problem, a practical engineering method has been performed, which is based on hybridizing simulation modeling with an optimization algorithm. Moreover, the sampling average approach for sizing and optimization of hybrid energy systems is employed to handle the challenges related to existing uncertainties.

3. Proposed approach

This study intends to provide an engineering tool based on a simulation-based optimization approach for the proposed design problem. For this purpose, a stochastic multi-objective optimization model is developed for the mentioned design problem. The capacity of the components and the allocation coefficients of the technologies to meet heating, cooling, electricity, and transportation load are defined as decision variables. The below vectors contain the summary of decision variables of the model:

$$\vec{P} = [P_{PV}, P_{WT}, P_{SC}, P_{HP}, P_{HST}, P_{Bio}, P_{PVR}] \quad (1)$$

$$\vec{\varepsilon} = [\varepsilon_{HE,HP}, \varepsilon_{HE,bb}, \varepsilon_{CO,HP}, \varepsilon_{CO,AR}, \varepsilon_{Tr,PEV}, \varepsilon_{Tr,gas}] \quad (2)$$

Three objective functions are to minimize total NPC, maximize RER, and minimize CO_2 emission. These objectives are subjected to a desirable level of reliability and other technical constraints which introduce the physical concept of the problem. The subsequent section introduces the mathematical formulation of the three objective functions. Readers are referred to the previous work for more details of the optimization problem formulation and the constraints mathematical formulation [19].

In this study, investment cost of components, their operation and maintenance cost, as well as their replacement cost are marked as total NPC. Additionally, it composes of fuel cost, rental cost of the land, biomass collection, storage and transportation cost over the project life time, Eq. (3) [19].

$$\begin{aligned} NPC = \sum_j \left[C_{I,j} + C_{O\&M,j} \frac{1}{CRF(i,T)} + C_{rep,j} K_j \right] P_j \\ + \{ C_{elec,b} E_{bought} + C_{NG} NG_y - C_{elec,s} E_{Sold} + C_{Gas}(\text{Gasoline}) \\ + \text{Biomass}_y (C_{b,Col} + C_{b,St} + C_{b,Tr}) \} \frac{1}{CRF(i,T)} \end{aligned} \quad (3)$$

One aim of this study is to inspect the possible approaches to increase renewable resource utilization. A simple way to quantify this is to calculate the renewable energy ratio. It demonstrates the corresponding shares of renewable and non-renewable sources of energy consumption. There is a simple definition for RER which can be used for the future energy planning of communities. The formula below (Eq. (4)) is applied for calculating RER. It is defined as the ratio of total used renewable energy and total used primary energy [19].

$$RER = \frac{\text{Renewable energy}}{\text{Primary energy}} \quad (4)$$

The environmental criterion that is being considered in the optimization problem is to minimize pollution emission. In order to quantify the amount of produced pollutants, CO_2 is assumed as the only pollution emission since it is the main cause of emission. The CO_2 is emitted by gasoline cars, natural gas boiler, and it is resulted from the electricity bought from the grid, Eq. (5) [19].

$$CO_2 = (\text{Gasoline}) EF_{Gas} + NG_y EF_{NG} + E_{bought} EF_E \quad (5)$$

The maximum level for loss of load probability (LLP) is applied in a constraint that the designed system should satisfy its desired level, Eq. (6). LLP is defined as the total unmet energy divided by total energy load, Eq. (7) [19].

$$LLP < LLP_{max} \quad (6)$$

$$LLP = \frac{\text{Unmet load}}{\text{Load}} \quad (7)$$

3.1. Sampling average method

In this study, the sampling average method (SAM) is applied to tackle the existing randomness and consequently to approximate the objective functions. In order to acquire a model that is able to tackle the randomness, the most popular way is to optimize the expected value of an arbitrary function of the parameters, which is

defined over an appropriate probability space. Suppose a multi-objective stochastic optimization problem as following [21]:

$$\text{Min } \{ F_1(x), F_2(x), \ldots \} \quad \text{Subject to } x \epsilon S \tag{8}$$

In which, $F_v(x)$ is estimated by $\mathbb{E}(f_v(x,\omega))$, where, $v=(1, 2, \ldots)$, S defines the bound of decision space, and ω reflects the randomness effect. Let $\omega_1, \ldots, \omega_N$ as N random scenarios that are all independent, the sample average estimation of $F_v(x)$ can be calculated by [21]:

$$\frac{1}{N}\sum_{v=1}^{N} f_\vartheta(x,\omega_v) \approx \mathbb{E}(f_\vartheta(x,\omega)) \tag{9}$$

The basic idea of SAM is to replace the expected value function with its corresponding approximation, Eq. (9), and then find a solution for the derived deterministic model. By a similar way, the expected value of functions in a multi-objective optimization problem can be replaced by their sample average approximations to compute an estimation of their solution. Thusly, the following deterministic multi-objective problem is resulted, Eq. (10) [21].

$$\text{Min } \left(\frac{1}{N}\sum_{v=1}^{N} f_1(x,\omega_v), \ \frac{1}{N}\sum_{v=1}^{N} f_2(x,\omega_v), \ \ldots \right) \tag{10}$$

Typically, it is a complex task to exactly compute the expected value in the problem represented by Eq. (8) that is why the approximation method is needed. In fact, Eq. (10) is an approximation for the original problem of Eq. (8). Hence, a solution algorithm produces a set of arbitrary and independent samples to estimate the expected value of the objective functions. Then, the complex stochastic problem is converted to a deterministic problem which can be solved by either exact algorithm, or alternatively by a (multi-objective) meta-heuristic to determine a PF for the given problem [21]. In this study, DMOPSO is used as the solution method [21].

3.2. The synthetic generation of the random parameters

3.2.1. Wind speed

In this study, the methodology that is proposed by Dufo-López et al. [22] is used to reproduce hourly wind speed data. The idea of the model is simple as described in Eq. (11) in which the hourly wind speed data ($w_{d,h}$) is calculated [22].

$$w_{d,h} = e_{d,h} . f_{\text{correction}-m} \tag{11}$$

where $e_{d,h}$ is obtained by subtracting a fraction of the average monthly value ($w_{av,m}$) from the value of $c_{d,h}$, Eq. (12). When a negative value is resulted by Eq. (12), it must be set as zero. $f_{\text{correction-}m}$ is named correction factor and it is calculated by Eq. (13). Its role is to check that monthly average of measured data is the same as the estimated wind speed data.

$$e_{d,h} = c_{d,h} - f_{\text{substract}} \cdot w_{av,m} \tag{12}$$

$$f_{\text{correction}-m} = w_{av,m} \cdot 24 \cdot d_m / \sum_{\text{month}} e_{d,h} \tag{13}$$

where $w_{m,h}$ denotes the average of wind speed for an hour (h: $0 \le h \le 23$) in the month m, which is computed by Eq. (14); d_m is the number of days in the month m; $c_{d,h}$ stands for the hourly correlated values of each day, Eqs. (15) and (16) [22].

$$w_{m,h} = w_{n,m} + \text{Max}\,[0, \ (A_m - F_m . (t - h_{\max,m})^2] \tag{14}$$

where F_m is a factor providing information about the relation between the time of day and wind speed; A_m is the monthly amplitude; $h_{\max,m}$ is the hour that maximum speed in a day is occurred; and $w_{n,m}$ is the average monthly night speed [22].

$$\text{If}(d=0 \& h=0): \ c_{d,h} = \text{Weibull}_{d,h} \tag{15}$$

$$\text{Else}: \quad c_{d,h} = fc \cdot c_{d,h-1} + (1-fc) \cdot \text{Weibull}_{d,h} \tag{16}$$

where $\text{Weibull}_{d,h}$ is a random number which is generated by a Weibull distribution function with b form factor and the scale factor of θ_h, Eqs. (17) and (18) [22].

$$\text{Weibull}_{d,h} = [-\theta_h^b \cdot \ln(1-a_{d,h})]^{1/b} \tag{17}$$

where $a_{d,h}$ indicates a random number in range of (0–1).

$$\theta_h = w_{m,h} / \Gamma(1+\frac{1}{b}) \tag{18}$$

where $\Gamma(1+1/b)$ is the Gamma function. In order to control that the monthly average of measured data is the same as desired values, the cumulative distribution function of both generated series and the Weibull distribution function are compared [22]. In this study, f_c is assumed 0.9 and f_{subtract} is set at 0.8 [22].

3.2.2. Solar radiation

With the collected data, a mathematical model is developed to generate random hourly solar radiation, Eq. (19). The solar radiation is divided into two parts deterministic part and random part.

$$I_h = \mu_h + \varepsilon_h \tag{19}$$

where I_h is the solar radiation of the model; μ_h is the average of solar radiation for hour h which represents the average of hourly historical data. In other words, it is identified by making average for each hour of historical data. ε_h is a random number that is approximated by a normal distribution function. The distribution function is resulted by fitting the function on hourly standard deviation of solar radiation.

3.2.3. Ambient temperature

According to Krenzinger et al. [23], the ambient hourly temperature can be estimated by adding one random part (δ) to a periodic term (PT), a solar term (ST) and a base term T_{base}; Eq. (20) shows their model [23]:

$$T(t) = T_{\text{base}}(t) + PT(t) + ST(t) + \frac{\delta}{2} \tag{20}$$

The following section describes the mathematical model for three mentioned terms. In order to define the base term of temperature, a linear interpolation is used as it is shown in Eq. (21). There is an experimental term for the purpose of adjusting the mean of final result [23].

$$T_{\text{base}}(t) = T_{\text{mean}}(\text{day}) + (t+1)\frac{T_{\text{mean}}(\text{day}+1) - T_{\text{mean}}(\text{day})}{24} - [1 + 0.155A(\text{day})] \tag{21}$$

where $T_{\text{mean}}(\text{day})$ is the mean daily temperature which is identified by Eq. (22) [23].

$$T_{\text{mean}}(\text{day}) = T_{\text{base}}(\text{day}) + SD \tag{22}$$

$$SD = 4.2 - 0.15(T_{\min,m}) \tag{23}$$

The base temperature $T_{\text{base}}(\text{day})$ is defined by Eq. (24); $A(\text{day})$ is named daily amplitude of temperatures as seen in Eq. (25).

$$T_{\text{base}}(\text{day}) = \frac{1}{3}(T_{\text{mean},m}) \left[2 + \frac{H_0(\text{day})}{H_0(\text{month})} \right] \tag{24}$$

where $H_o(\text{day})$ is the extraterrestrial solar radiation in a given day and $H_o(\text{month})$ is the monthly averaged daily extraterrestrial solar radiation. $T_{\min,m}$, $T_{\max,m}$ and $T_{\text{mean},m}$, respectively, give the monthly averaged

minimum, maximum and mean ambient temperature [23].

$$A(\text{day}) = (I_{\max}(\text{day}) - I_{\max,m}) \left[\frac{A_{\max,d} - A_{\text{mean},d}}{I_{\max}(\text{month}) - I_{\max,m}} \right] + A_{\text{mean},d} + \delta \quad (25)$$

$I_{\max}(\text{day})$ is the value of maximum solar radiation for each day; $I_{\max,m}$ is the monthly average of maximum solar radiation for each day; $I_{\max}(\text{month})$ is the maximum value of solar radiation in whole the month; $A_{\text{mean},d}$ and $A_{\max,d}$ are mean and maximum daily amplitude, respectively, those are calculated by Eqs. (26) and (27) [23].

$$A_{\text{mean},d} = T_{\max,m} - T_{\min,m} \quad (26)$$

$$A_{\max,d} = 25 - 0.42(T_{\min,m}) + \frac{\delta}{2} \quad (27)$$

where δ is a random variable uniformly distributed between -1 and $+1$. Eqs. (28) and (29) are used to examine the periodic term according to the time of a day. The first equation is related to time before sunrise and the next one is assigned for time after t_{sr} [23].

$$\text{If} \quad t < t_{sr} \quad \text{then} \quad PT(t) = \frac{A(\text{day})}{4} \left\langle \frac{1}{2} + \text{COS}\left(\frac{(20+t)\pi}{20 - t_{sr}\,2} \right) \right\rangle \quad (28)$$

$$\text{Else} \quad PT(t) = \frac{A(\text{day})}{8} \left\langle \text{COS}\left(\frac{(16-t)\pi}{15 - t_{sr}\,2} \right) + \text{COS}\left(\frac{(14-t)\pi}{13 - t_{sr}\,2} \right) \right\rangle \quad (29)$$

The solar term is then determined through a simple equation in which the maximum temperature $T_{\max}(\text{day})$, a recurrent term (Δ), and the time of the maximum solar radiation are the main terms, Eq. (30) [23].

$$ST(t) = \left\langle \frac{T_{\max}(\text{day}) - [T_{\text{base}}(t) + PT(15)]}{I_{\max}(\text{day})} + \Delta \right\rangle I(t-1) \quad (30)$$

The maximum temperature in the day is evaluated through adding a half of daily amplitude to the mean daily temperature, as seen in Eq. (31) [23].

$$T_{\max}(\text{day}) = T_{\text{mean}}(\text{day}) + \frac{A_{\max}(\text{day})}{2} \quad (31)$$

After generating hourly temperature for a day, a comparison between the resulted mean temperature and input data will be performed based on Eq. (32) to updated the Δ, and then iteration is repeated for daily generation[23].

$$\text{If} \quad \left(T_{\text{mean}}(\text{day}) - \sum \frac{T(t)}{24} \right) > 0.5 \quad \text{then}$$

$$\Delta = \Delta + \frac{T_{\text{mean}}(\text{day}) - \sum \frac{T(t)}{24}}{I_{\max}(\text{day})} \quad (32)$$

3.2.4. Load

In the feasibility study of renewable energy systems, it is required to develop a simple method to identify an energy load profile. A cluster analysis approach that is proposed in [24] has been applied for the purpose of generating electric and hot water load profile. For a representative building, the daily information of appliances such as their utilization, energy consumption, ownership, and occupied duration is used to produce daily load profile [24].

Table 2
Occupancy pattern for a three-person household [24].

Scenarios	Occupied period
1	0–9:00 & 13:00–23
2	0–9:00 & 18:00–23
3	0–9:00 & 16:00–23
4	0–24
5	0–13:00 & 18:00–23

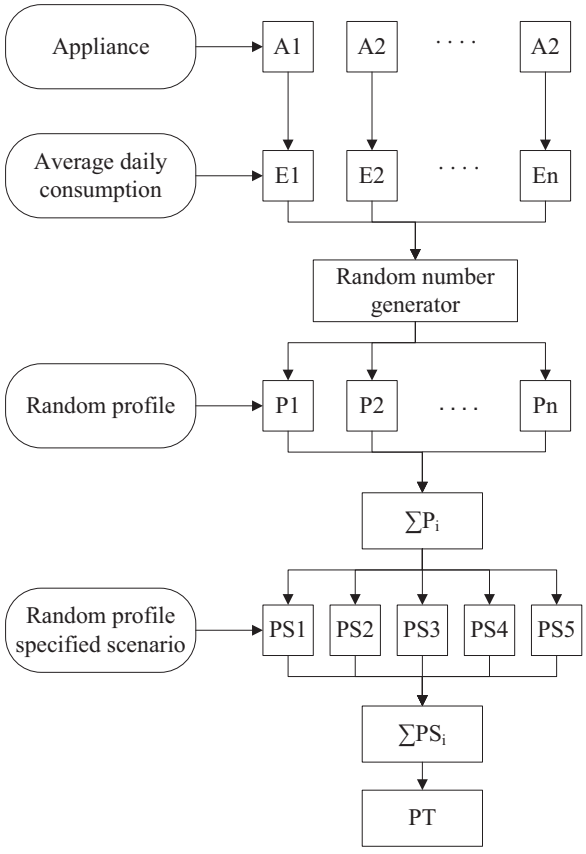

Fig. 2. Framework of generating the electricity or hot water load profile.

As the load profile is directly related to the occupation pattern of the buildings, it can be a promising task to identify the building clusters [24]. In this study, five most common scenarios of building occupancy pattern are considered since there is a lack of information [24]. In Table 2 these five scenarios are represented [24].

To evaluate the daily energy and hot water load profile, first, an average daily consumption of each appliance is determined based on monthly energy bill and the annul Canadian appliance energy consumption [25]. Fig. 2 represents the schematic of load profile generation process. For a specific scenario, a random load profile for appliances is generated according to a random number generator technique. By adding the random load profile of all appliances, the load profile of a specified scenario is produced produce which named “Specific Profile” since it is resulted from a certain occupation scenario [24]. The daily load profile of a specific scenario can change over different days. The random generation is repeated 20 times to return an approximately smooth load curve for a given day [24]. A specific load profile cannot reflect the general load profile for the building since it represents only one certain scenario of occupancy pattern. Hence, five specific profiles resulted by five scenarios are aggregated to produce a typical load profile for the electricity, hot water, and required energy for transportation of the building.

In Fig. 2, A_i is appliances name; E_i is the average daily energy consumption of the appliances; $P1$, $P2$, …, Pn describe random profiles those are generated for the appliances; PS_i is related to the specific profile corresponding to a particulate occupancy scenario; PT is a typical load profile [24]. It is worth mentioning that the heating and cooling load is approximated by degree hour [19] while other types of energy demand are estimated by using the mentioned methodology.

4. Solution approach

In order to solve the mentioned stochastic multi-objective optimization problem, a simulation-based optimization approach is used to generate a Pareto front. This approach is trying to apply simultaneously the advantage of simulation and optimization methods. In complicated systems, it is difficult to handle the model uncertainties and non-linearity with a stand-alone optimization method since it requires the precise mathematical model of the system. In these cases, the simulation can be considered as a powerful assessment engine to precisely contain all details of the system and involve existing uncertainties [26]. However, simulation suffers from the fact that it is inherently unable to return the optimal solution of the problem. Thus, the integration of these two methods can be an efficient solution approach when the optimization problem is complex due to either existing uncertainties or non-linear terms.

In this study, the simulation module accommodates the mathematical models for the components of the employed system (see Fig. 1). The main role of the simulation module is to check the feasibility of each candidate solution proposed by the optimization algorithm. The utilized optimization algorithm is developed based on the Particle Swarm Optimization (PSO) approach. Recently, PSO is implemented for multi-objective optimization problems since it was performed successfully in single objective problems [27]. This type of algorithms is named Multi-Objective Particle Swarm Optimization (MOPSO) [27]. In MOPSO a set of solutions named non-dominated solutions or Pareto front is derived instead of single solution resulted by PSO. In this study, MOPSO is extended to dynamic multi-objective particle swarm optimization (DMOPSO) algorithm which was developed in the previous work of the authors [27]. By using DMOPSO a promising improvement in the quality of garneted PF is obtained compared with well-known MOP approaches. The difference between the employed algorithm and MOPSO is that multi-leaders and dynamic cell-based density calculation strategy is utilized in the performed algorithm to update the solutions [27]. For detail explanation of the algorithm, readers are referred to the previous work [27].

5. Results and discussion

In order to evaluate the proposed methodology, a case study is selected which is located in Winnipeg, Canada. The case study is an apartment that contains 12 two-bedroom units and 31 one-bedroom units, and its total floor area and foot print is approximated by 2940 m^2 and 980 m^2, respectively. The current energy consumption of the building includes natural gas, grid-electricity and gasoline. In other words, a natural gas boiler is in charge of supplying heating load and hot water demand while the cooling load is met by air refrigerators. The building residences use gasoline to provide energy of their cars. In addition, the required electricity for appliance is satisfied by hydroelectricity which is bought from the grid. The primary RER of the building is estimated as 10% and the total GHG production is calculated as 277.1 (t/year) [19]. The average monthly energy use of the building is represented in Fig. 3 per type of energy carriers.

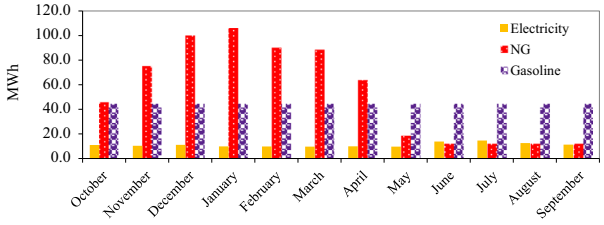

Fig. 3. Monthly energy consumption of the building per type of energy carrier [19].

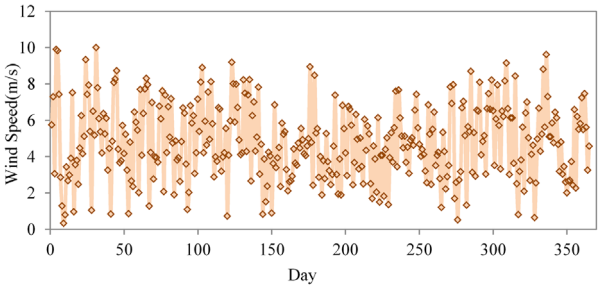

Fig. 4. Daily average hourly wind speed for Winnipeg.

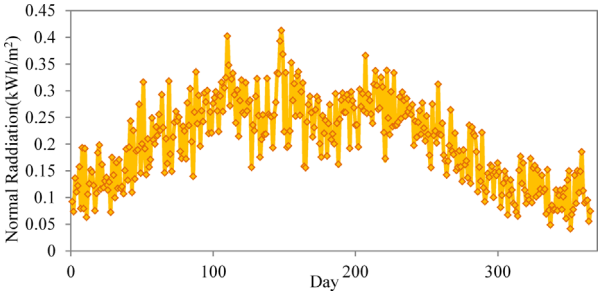

Fig. 5. Daily average hourly normal irradiation for Winnipeg.

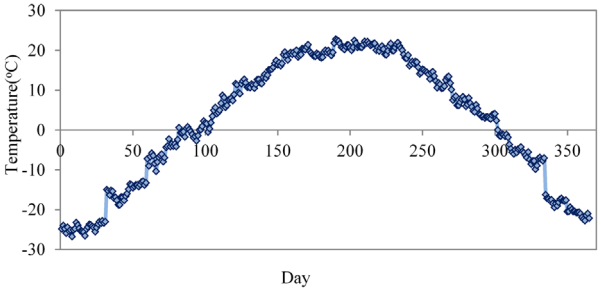

Fig. 6. Daily average hourly ambient temperature for Winnipeg.

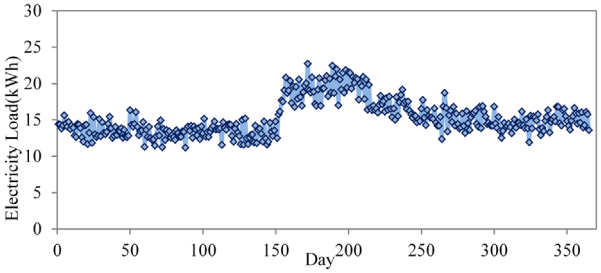

Fig. 7. Daily average electricity load of the building.

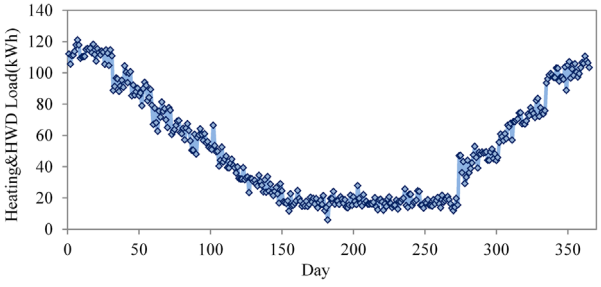

Fig. 8. Daily average hourly heating load for heating and hot water purpose of the building.

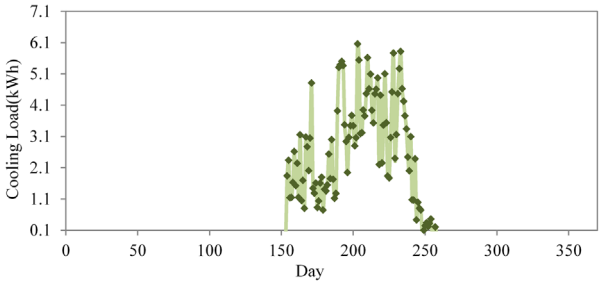

Fig. 9. Daily average hourly cooling load of the building.

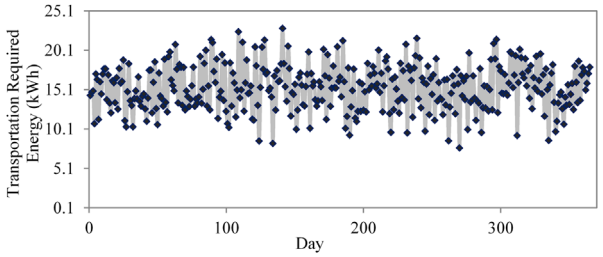

Fig. 10. Daily average hourly required energy for the transportation of the building.

The daily average hourly wind speed at 10 m height, direct normal irradiance, and ambient temperature over one year for the location are plotted in Figs. 4–6. These figures include stochastic data which is generated by the mentioned models in Section 3.2 while the deterministic one is obtained by averaging the measurement data over 15 years (1990–2004) [28]. In Figs. 4–10, the data represented and labelled as stochastic are the result of stochastic model over one sample year. It is worth mentioning that in these graphs, the day 0 represents the first day of January.

Similarly, Figs. 7–10 depict the required energy for different purposes (heating, cooling, HWD, electricity, and transportation) used in the stochastic model. In order to estimate the cooling and heating load, the concept of the degree-day is utilized in which it is assumed that the energy requirement for heating and cooling are directly depend upon the difference between base and outside temperature. In the deterministic model, the hourly input data over one year is entered to the model and stay constant over simulation run while the data in stochastic model is varying over years through the simulation run.

In this study, the economic parameters and characteristics of components such as the initial cost, operation and maintenance cost are considered the same as what has been exhibited in the previous work [19]. The employed HRES is implemented on the hourly basis in the simulation program which is coded by using C++ programming environment and executed in a 2.40 GHz Core 2 processor with 4 GB of RAM.

The Pareto fronts evolved using the proposed DMOPSO for the stochastic and deterministic design approaches are shown in Figs. 11–13, which show an illustration of the trade-off solutions. These figures show the comparison between stochastic and deterministic PFs. Besides, the descriptive non-dominated solutions evolved in the stochastic and deterministic cases are listed in Table 3. These solutions are tagged with numbers in Figs. 11–13. In Fig. 11, RER is outlined on the vertical axis and the curves show different value of NPC needed to obtain a design with corresponding RER value. Similarly in Fig. 12, the curves illustrate the total net present cost required to gain the corresponding value of CO_2 emission. It is evident that the total NPC has shifted to higher level in the stochastic case when it is compared to the deterministic design surface. In addition, Fig. 13 describes the trade-off solutions between RER and CO_2 emission. When the uncertainties are incorporated, this analysis helps us to reach up to

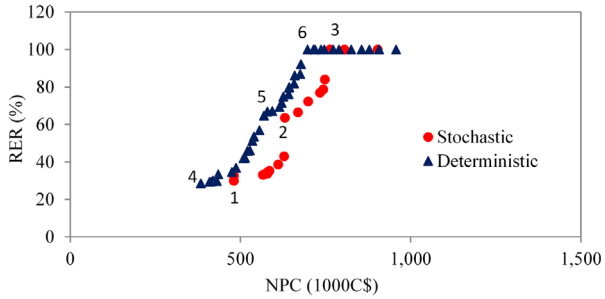

Fig. 11. The 2D Pareto front of the deterministic and stochastic design; RER vs NPC.

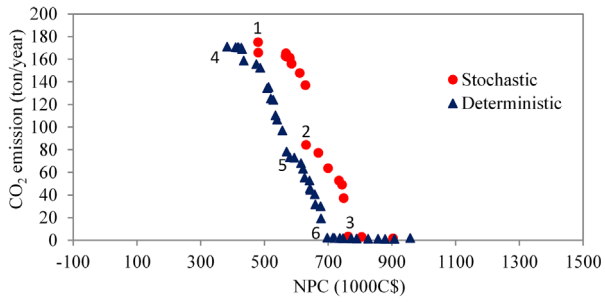

Fig. 12. The 2D Pareto front of the deterministic and stochastic design approaches; CO_2 emission vs NPC.

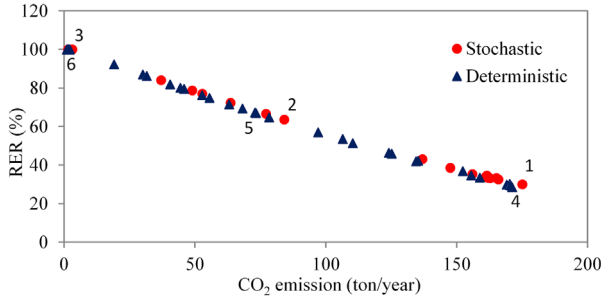

Fig. 13. The 2D Pareto front of the deterministic and stochastic design approaches; RER vs CO_2 emission.

90% increasing in RER and with up to 99.3% less CO_2 emission than the base case. The high RER and low emission region involve high total net present cost. There are some low NPC points but these involve low RER and high emission. As seen over stochastic curves in Figs. 11–13, that is relatively a costly option to increase RER from 29.9% to 63% since that requires 31% more NPC than the design configuration represented by the solution 1. Furthermore, by moving from solution 1 toward solution 2, the CO_2 emission is reduced moderately which is less than 52% or 84.2 (t/year). Between solution 2 and 3, the NPC would change moderately (less than 20%) while the value of RER is increased by 37%. Note that the most likely region of RER for the stochastic surface is between 29–80% and while for the deterministic PF solutions are distributed uniformly in range of 27–100%. This can be associated with the non-linearity of the model as well as it justifies considering uncertainty analysis. In the stochastic case, it is clear from the depicted PFs that the RER can reach to 100% through different solutions. That is, there are some options for RER of 100%, in which the NPC and CO_2 emission is varied. Over these solutions CO_2 emission is reduced slightly from 3.2 t/year to 2.6 t/year while total NPC is increased more than 18%. Hence, between solutions with the same RER of 100%, it is more reasonable that a solution with less NPC (solution 3) would be selected since there is no remarkable difference between their CO_2 emissions.

Table 3
Example solutions laying over the generated PF in the stochastic and deterministic cases.

Generators/Objectives	Stochastic			Deterministic		
	Solution 1	Solution 2	Solution 3	Solution 4	Solution 5	Solution 6
PV [kW]	0	0	0	0	0	0
Wind turbine [kW]	94	105	116	68	71	73
Solar collector [kW]	25	0	0	0	0	0
Heat pump [kW]	0	0	0	0	0	0
Heat storage tank [m^3]	4.3	4.3	4.3	4.3	4.3	4.3
Biomass boiler [kW]	0	95	200	0	91	200
PV-rural area [kW]	0	0	0	0	0	0
$\varepsilon_{HE,HP}$	0	0	0	0	0	0
$\varepsilon_{HE,bb}$	0	0.3	1	0	0.4	1
$\varepsilon_{CO,HP}$	0	0	0	0	0	0
$\varepsilon_{CO,AR}$	1	1	1	1	1	1
$\varepsilon_{Tr,PEV}$	0.94	1	1	1	1	1
$\varepsilon_{Tr,gas}$	0.06	0	0	0	0	0
LLP [%]	4.8	4.8	4.8	5	4.9	4.9
NPC [C$]	480265	630741	763062	383284	579654	705180
RER [%]	30	63	100	28.5	67	100
CO_2 emission [ton/yr]	175.1	84.2	3.2	171.2	73.4	2.4

Table 4
The bound of different objectives obtained by stochastic and deterministic optimization approaches.

	Minimum		Average		Maximum	
	Stochastic	Deterministic	Stochastic	Deterministic	Stochastic	Deterministic
RER [%]	29.9	28.5	56.2	63	100	100
Emission [ton/yr]	1.6	1.1	106.5	87.3	175	171.2
NPC [1000C$]	480.2	383.3	646.3	595	903.4	957

In this type of portrayal, decision makers can conveniently distinguish the minimum NPC, CO_2 emission, or maximum possible RER that can be achieved by this graph. That is, based on decision maker's desire, a convenient solution can be selected from a set of non-dominated solutions. By retracting one step, the value of decision variables can be found where we need to install those capacities to obtain these kinds of performances.

The Pareto front attained as the result of deterministic optimization scheme is also presented in Figs. 11–13. As shown, there is no significant different in PFs shape while there is moderate different in level between the deterministic and stochastic PF surfaces. The maximum, minimum, average of performance criteria for non-dominated solutions laying over the stochastic and deterministic PF surfaces are summarized in Table 4.

There is a slightly difference (less than 9%) between the average total NPC of two cases. Additionally, the range of RER and CO_2 emission that stochastic PF is able to enclose is competitive to the deterministic case. The total NPC in stochastic design shows a higher shift as the deterministic design is based on the average values of historical data while stochastic evaluate more realistic situation. In this regards, the decision variables are distinctive for two cases as shown in Table 3. For instance, in the maximum RER case, the installed capacity of the wind turbine in the deterministic approach is less than the stochastic one. In the minimum RER designs, the stochastic solution (see solution 1 in Table 3) use wind turbine, SC, and PEV while deterministic one only employs wind turbine and PEV. Correspondingly, this reduces total NPC more in deterministic case than stochastic case which changes the non-dominated solutions surface.

Furthermore, the quality analysis of generated Pareto fronts in the stochastic and deterministic cases is performed using the well-known performance metrics. For this purpose, three metrics are employed which are named spacing metric, diversification metric, and set coverage metric [27]. The spacing metric is used to measure the distribution of individuals over PF while diversification metric determines the maximum extension that can be covered by non-dominated solutions [27]. The set coverage metric is applied to compare two given PFs and identify the closet PF to the optimal PF [27]. The readers are referred to the previous work of this study [27] for more details about the PF performance metrics definition and their mathematical calculation. Table 5 shows the comparison between the deterministic and stochastic PFs by using three performance metrics, obtained PF size, and running time of the algorithms.

Table 5
The performance metric value for the stochastic and deterministic problem.

Performance metric	Stochastic	Deterministic
Spacing	0. 14	0.09
Diversification	4.24	4.96
PF size	20	42
Time (Second/iteration)	308	28
SC (Stochastic, Deterministic)	0%	
SC (Deterministic, Stochastic)	55%	

It seems the inclusion of uncertainties has decreased the range of objective function almost for RER and CO_2 emission, thereby providing less flexibility to designer. This fact can be clearly inferred from the diversification metric result since this metric has slightly better outcome in the deterministic case. The spacing metric of the stochastic case is greater than the deterministic case. It means the solutions over deterministic PF are distributed more uniform. The set coverage metric clearly shows the dominance of the deterministic over stochastic PF. It represents that 55% of solutions placed over the stochastic PF are dominated by the solutions resulted by the deterministic PF. Here, the set coverage metric is used to show that some of solutions of the PF generated

by the stochastic model are shifted to higher NPC, less RER, and higher CO_2 emission. It is not relatively reasonable to compare these two obtained PFs based on the set coverage metric as the input data is notable different in the stochastic and deterministic cases. The PF size of the deterministic case is almost two times of the stochastic PF size. The time needed to solve the stochastic problem is increased significantly (more than 11 times) compared to the deterministic case. It can be concluded that the performance of DMOPSO in the deterministic optimization problem is prominent than the stochastic case. It means that when the system randomness is incorporated, the efficiency and effectiveness of DMOPSO in the developed multi-objective optimization problem is reduced. Nevertheless, stochastic analysis result is preferred over the deterministic one since it examines a significant range of possible future outcomes and consequently its results are more realistic. In other words, the stochastic optimization helps decision makers to choose a solution that is evaluated in a condition closer to the real life situation than what is predefined in the deterministic design.

Finally, sensitivity analysis is implemented to assess the impact of changing the values of parameters on the derived PF. In order to carry out the analysis, 13 parameters are considered, and then upper and lower limits for the parameters are examined to study their effect on the resulted PF. The studied parameters are summarized in Table 6.

The parameters are set in their upper and lower limits to illustrate the change in the average of NPC of the solutions with RER of 100%, Fig. 14. The average of total NPC and CO_2 emission of the solutions with RER of 100%, which are laying over the original stochastic PF (see Figs. 11–13) are estimated as C$ 824039 and 2.61 (t/year), respectively. Fig. 14 shows the changes in total NPC where the studied constants are fixed at their upper or lower limits. For example, the interest rate is reduced by 50%, then the changes in the average of total NPC of solutions with the highest RER are monitored which are 12.9% higher than the value of the base case.

Table 6
Studied parameters in the sensitivity analysis.

Parameters	Abbreviation	Parameters	Abbreviation
Biomass transportation cost	BioT	Sold electricity price	SoEP
Biomass collection cost	BioC	Wind turbine capital cost	WTC
Biomass storage cost	BioSt	Solar collector capital cost	SCC
Land rental cost	LaC	Heat pump capital cost	HPC
Gasoline price	GaP	PV panel capital cost	PVC
NG price	NGP	Interest rate	IR
Grid electricity price	GEP		

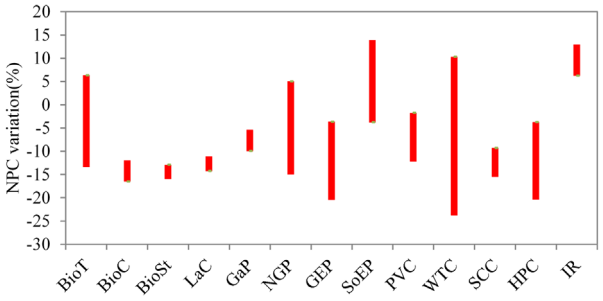

Fig. 14. Sensitivity analysis result; NPC variation versus the parameters variation.

In order to perform the sensitivity analysis, DMOPSO is run 5 times to identify the standard deviation of the average of objectives. It observes that the standard deviation of the average of NPC is set at 16.2%. In the inferring of the sensitivity analysis result, if the differences between an objectives function and its original values would be less than its standard deviation that can be neglected. As it is obvious from the result, wind turbine capital cost and electricity and price, have more effect on total NPC than others. It is clear from Fig. 14 that changing the solar collector and PV panels capital cost resulted in a small variation of NPC as there is small contribution for them in the obtained non-dominated solutions.

6. Conclusion

In this study, simulation-based optimization approach is proposed to solve optimal sizing of HRESs taking into considerations the uncertainties existing in RE resources and energy demand. A dynamic multi-objective particle swarm optimization (DMOPSO) algorithm, simulation module, and sampling average technique are used to derive out a set of non-dominated solutions for an HRES applied to buildings where multiple energy sources are used.

The proposed method applies synthetic data generation to provide data series for wind speed, solar irradiance, ambient temperature, and energy load. The sampling average technique integrated with the simulation module is in charge of handing the complexity resulted by incorporating uncertainties. In the developed multi-objective optimization problem, three design criteria are considered including total net present cost of the system, renewable energy ratio, and CO_2 emission where a desirable level of loss of load probability should be satisfied. A set of renewable energy technologies is assessed in order to increase the RER of an apartment building located in Canada. The employed renewable energy technologies contain PV panels, wind turbines, heat pumps, biomass boilers, and PEV cars. In order to evaluate the performance of the proposed approach, the obtained Pareto front is compared with the deterministic PF through well-known performance metrics. The result shows that RER can be increased by 100% in both cases while a higher NPC is observed in the stochastic case. In addition, the employed performance metric outcomes show that the quality of the generated PF in the deterministic case is better than the stochastic one. However, stochastic analysis result is more desirable since it examines a significant range of possible future outcomes and consequently its results are more informative and realistic. The sensitivity analysis is performed to identify the economic parameters that have more significant effect on the design criteria. Its finding describes that wind turbine capital cost, and electricity price, have most impact on total NPC.

For future research directions of the present work, hybridization methods based on local search techniques can be used to increase the efficiency and effectiveness of DMOPSO algorithm in the application of the stochastic multi-objective optimization problem. The DMOPSO can be modified to find a PF in a more reasonable time since the incorporation of uncertainties increases the complexity of the problem.

Acknowledgment

The authors acknowledge the funding received from the NSERC discovery grant (315104) and the University of Manitoba Graduate Fellowship (UMGF) to support this research.

References

[1] Ekren O, Ekren BY. Size optimization of a solar-wind hybrid energy system using two simulation based optimization techniques. In: Carriveau DrRupp, editor. Rijeka, Croatia: INTECH Open Access Publisher; 2011.

[2] Thompson S, Duggirala B. The feasibility of renewable energies at an off-grid community in Canada. Renewable Sustainable Energy Rev 2009;13(9):2740–5.
[3] Rosiek S, Batlles FJ. Renewable energy solutions for building cooling, heating and power system installed in an institutional building: case study in southern Spain. Renewable Sustainable Energy Rev 2013;26:147–68.
[4] Akella AK, Sharma MP, Saini RP. Optimum utilization of renewable energy sources in a remote area. Renewable Sustainable Energy Rev 2007;11 (5):894–908.
[5] Banos R, Manzano F, Montoya FG. Optimization methods applied to renewable and sustainable energy: a review. Renewable Sustainable Energy Rev 2011;15 (4):1753–66.
[6] Abedi S, Alimardani A, Gharehpetian GB, Riahy GH, Hosseinian SH. A comprehensive method for optimal power management and design of hybrid RES-based autonomous energy systems. Renewable Sustainable Energy Rev 2012;16(3):1577–87.
[7] Maheri A. Multi-objective design optimization of standalone hybrid wind-PV-diesel systems under uncertainties. Renewable Energy 2014;66:650–61.
[8] Arun P, Banerjee R, Bandyopadhyay S. Optimum sizing of photovoltaic battery systems incorporating uncertainty through design space approach. Sol Energy 2009;83:1013–25.
[9] Dufo-lópez R, Bernal-agustín JL, Lujano J, Domínguez-navarro JA. Utilization of synthetically generated hourly wind speed data in the optimization of wind-batteries stand-alone systems. In: Proceeding of international conference on renewable energies and power quality, Las Palmas de Gran Canaria, Spain; 2011.
[10] Handschin E, Neise F, Neumann H, Schultz R. Optimal operation of dispersed generation under uncertainty using mathematical programming. Int J Electr Power Energy Syst 2006;28:618–26.
[11] Ekren O, Ekren BY. Size optimization of a PV/wind hybrid energy conversion system with battery storage using response surface methodology. Appl Energy 2008;85:1086–101.
[12] Ekren O, Ekren BY. Size optimization of a PV/wind hybrid energy conversion system with battery storage using simulated annealing. Appl Energy 2010;87:592–8.
[13] Giannakoudis G, Papadopoulos AI, Seferlis P, Voutetakis S. Optimum design and operation under uncertainty of power systems using renewable energy sources and hydrogen storage. Int J Hydrog Energy 2010;35:872–91.
[14] Khan MJ, Iqbal MT. Pre-feasibility study of stand-alone hybrid energy systems for applications in Newfoundland. Renewable Energy 2005;30:835–54.
[15] Kuznia L, Zeng B, Centeno G, Miao Z. Stochastic optimization for power system configuration with renewable energy in remote areas. Ann Oper Res 2012;210 (1):411–32.
[16] Roy A, Kedare SB, Bandyopadhyay S. Optimum sizing of wind-battery systems incorporating resource uncertainty. Appl Energy 2010;87:2712–27.
[17] Subramanyan K, Diwekar UM, Goyal A. Multi-objective optimization for hybrid fuel cells power system under uncertainty. J Power Sources 2004;132:99–112.
[18] Wang L. Integration of renewable energy sources: reliability-constrained power system planning and operations using computational intelligence. Texas A&M University; 2008.
[19] Sharafi M, ElMekkawy TY, Bibeau EL. Optimal design of hybrid renewable energy systems in buildings with low to high renewable energy ratio. Renewable Energy 2015;83:1026–42.
[20] Manitoba Hydro. Technical requirements for connecting distributed recourses to the Manitoba Hydro system, DRG 2003, Rev2, MBHydro Electric Board; 2010.
[21] Gutjahr WJ, Reiter P. Bi-objective project portfolio selection and staff assignment under uncertainty. Optimization 2010;59:417–45.
[22] Dufo-lópez R, Bernal-agustín JL. New methodology for the generation of hourly wind speed data applied to the optimization of stand-alone systems. Energy Procedia 2012;14:1973–8.
[23] Krenzinger A, Leite RS, Farenzena DS. Synthesizing sequences of hourly ambient temperature data. In: Proceedings of 17th international congress of mechanical engineering, Sao Paulo, Brazil; 2003.
[24] Yao R, Steemers K. A method of formulating energy load profile for domestic buildings in the UK. Energy Build 2005;37:663–71.
[25] NRC. Energy use data handbook tables. Natural Resources Canada, Canada, available from: ⟨http://oee.rncan.gc.ca/publications/statistics/handbook11/index.cfm⟩; 2014.
[26] Sharafi M, ELMekkawy TY. Multi-objective optimal design of hybrid renewable energy systems using PSO-simulation based approach. Renewable Energy 2014;68:67–79.
[27] Sharafi M, Elmekkawy TY. A dynamic MOPSO algorithm for multi-objective optimal design of hybrid renewable energy systems. Int J Energy Res 2014;38 (15):1949–63.
[28] Environment Canada—Atmospheric Environment Service and the National Research Council of Canada. Canadian weather energy and engineering data sets (CWEEDS Files), available from: ⟨http://climate.weather.gc.ca/prods_servs/engineering_e.html⟩; 2012.